Co-activation of AMPK and mTORC1 Induce Cytotoxicity in Acute Myeloid Leukemia

Pierre Sujobert, Laury Poulain, Etienne Paubelle, Florence Zylbersztejn, Adrien Grenier, Mireille Lambert, Elizabeth Townsend, Jean-Marie Brusq, Edwige Nicodeme, Justine Decrooqc, et al.

Article

Cell Reports

Co-activation of AMPK and mTORC1 Induce Cytotoxicity in Acute Myeloid Leukemia

Graphical Abstract

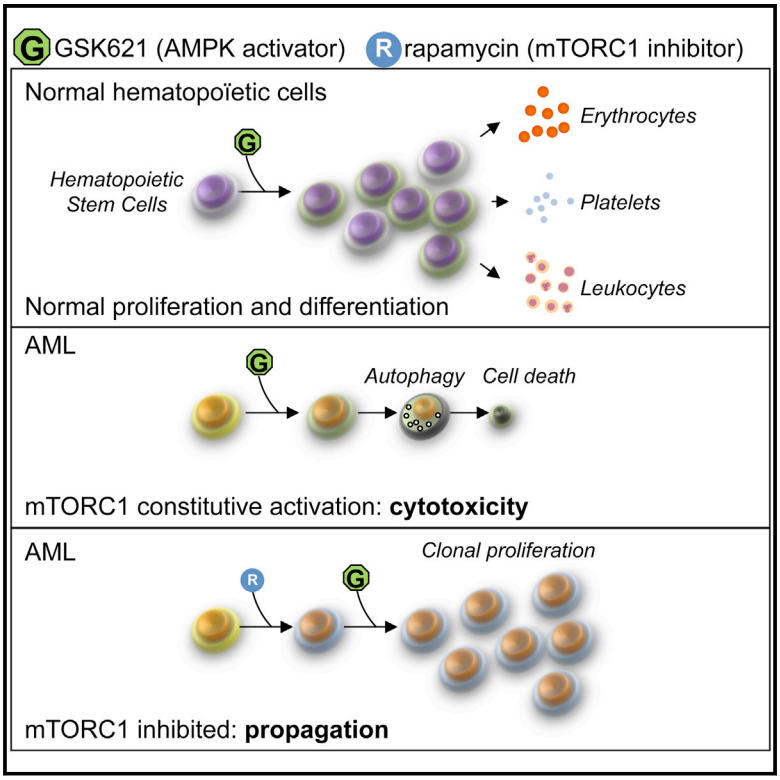

Highlights

- AMPK activation blocks AML propagation without toxicity to normal hematopoiesis
- Cytotoxicity induced by an AMPK activator (GSK621) involves autophagy in AML
- Co-activation of AMPK and mTORC1 is synthetically lethal in AML
- AMPK and mTORC1 crosstalk requires eIF2α/ATF4 signaling

Authors

Pierre Sujobert, Laury Poulain, ..., Didier Bouscary, Jerome Tamburini

Correspondence

jerome.tamburini@inserm.fr

In Brief

Sujobert et al. show that specific AMPK activation by GSK621 induces cytotoxicity in AML but not in normal hematopoietic cells. AMPK-mediated cytotoxicity indeed requires mTORC1 activation that is unique to AML cells and involves the eIF2α/ATF4 signaling pathway. This indicates a potential for AMPK-activating agents in the treatment of mTORC1-overactivated cancers.

Sujobert et al., 2015, Cell Reports *11*, 1–12
June 9, 2015
http://dx.doi.org/10.1016/j.celrep.2015.04.063

CellPress

Please cite this article in press as: Sujobert et al., Co-activation of AMPK and mTORC1 Induce Cytotoxicity in Acute Myeloid Leukemia, Cell Reports (2015), http://dx.doi.org/10.1016/j.celrep.2015.04.063

Cell Reports
Article

Co-activation of AMPK and mTORC1 Induce Cytotoxicity in Acute Myeloid Leukemia

Pierre Sujobert,[1,2,3,4] Laury Poulain,[1,2,3,4] Etienne Paubelle,[5,6,7,8] Florence Zylbersztejn,[5,6,7,8] Adrien Grenier,[1,2,3,4] Mireille Lambert,[1,2,3,4] Elizabeth C. Townsend,[9] Jean-Marie Brusq,[10] Edwige Nicodeme,[10] Justine Decrooqc,[5,6,7,8] Ina Nepstad,[11] Alexa S. Green,[1,2,3,4] Johanna Mondesir,[1,2,3,4] Marie-Anne Hospital,[1,2,3,4] Nathalie Jacque,[1,2,3,4] Alexandra Christodoulou,[9] Tiffany A. Desouza,[9] Olivier Hermine,[5,6,7,8] Marc Foretz,[1,2,3,8] Benoit Viollet,[1,2,3,8] Catherine Lacombe,[1,2,3,4] Patrick Mayeux,[1,2,3,4] David M. Weinstock,[9] Ivan C. Moura,[5,6,7,8] Didier Bouscary,[1,2,3,4] and Jerome Tamburini[1,2,3,4,*]

[1]INSERM U1016, Institut Cochin, 75014 Paris, France
[2]CNRS UMR8104, 75014 Paris, France
[3]Université Paris Descartes, Faculté de Médecine Sorbonne Paris Cité, 75005 Paris, France
[4]Equipe Labellisée Ligue Nationale Contre le Cancer (LNCC), 75013 Paris, France
[5]INSERM UMR 1163, Laboratory of cellular and molecular mechanisms of hematological disorders and therapeutic implications, 75015 Paris, France
[6]Paris Descartes–Sorbonne Paris Cité University, Imagine Institute, 75015 Paris, France
[7]CNRS ERL 8254, 75015 Paris, France
[8]Laboratory of Excellence GR-Ex, 75015 Paris, France
[9]Department of Medical Oncology, Dana-Farber Cancer Institute and Harvard Medical School, Boston, MA 02215, USA
[10]GlaxoSmithKline Research Center, 91490 Les Ulis, France
[11]Division for Hematology, Department of Medicine, Haukeland University Hospital, N-5021 Bergen, Norway
*Correspondence: jerome.tamburini@inserm.fr
http://dx.doi.org/10.1016/j.celrep.2015.04.063

SUMMARY

AMPK is a master regulator of cellular metabolism that exerts either oncogenic or tumor suppressor activity depending on context. Here, we report that the specific AMPK agonist GSK621 selectively kills acute myeloid leukemia (AML) cells but spares normal hematopoietic progenitors. This differential sensitivity results from a unique synthetic lethal interaction involving concurrent activation of AMPK and mTORC1. Strikingly, the lethality of GSK621 in primary AML cells and AML cell lines is abrogated by chemical or genetic ablation of mTORC1 signaling. The same synthetic lethality between AMPK and mTORC1 activation is established in CD34-positive hematopoietic progenitors by constitutive activation of AKT or enhanced in AML cells by deletion of TSC2. Finally, cytotoxicity in AML cells from GSK621 involves the eIF2α/ATF4 signaling pathway that specifically results from mTORC1 activation. AMPK activation may represent a therapeutic opportunity in mTORC1-overactivated cancers.

INTRODUCTION

Conventional chemotherapy for acute myeloid leukemia (AML) is curative in only a minority of patients, and toxicity limits its use in the elderly and in those with comorbidities (Büchner et al., 2012). Therefore, novel strategies that specifically target AML cells while sparing normal tissues are desperately needed. AMP-Activated Protein Kinase (AMPK) is a heterotrimeric serine/threonine kinase that acts as a sensor of cellular energy and modulates multiple cellular metabolic pathways (Hardie et al., 2012). In particular, activation of AMPK inhibits mammalian Target of Rapamycin Complex 1 (mTORC1)-dependent protein synthesis (Inoki et al., 2003), and also fatty acid biosynthesis via inactivating phosphorylation of acetyl-Coa carboxylase (ACC) (Fullerton et al., 2013). At the same time, AMPK also promotes catabolism, including glucose uptake and subsequent glycolysis, fatty acid oxidation, and autophagy (Hardie et al., 2012).

AMPK appears to act as either a tumor suppressor or an oncogene, depending on the context (Faubert et al., 2013; Jeon et al., 2012; Shackelford et al., 2009, 2013). The indirect AMPK activator metformin has activity in cell line models of AML (Green et al., 2010). However, the biological effects of biguanides such as metformin and phenformine in cancer primarily involve the general consequences of mitochondrial respiratory chain inhibition and are incompletely related to AMPK (Scotland et al., 2013; Shackelford et al., 2013).

In the present study, we tested the AMPK activator GSK621 in AML cells. We demonstrate that GSK621 is a direct and specific activator of AMPK that induces cytotoxicity by activating autophagy independent of mTORC1 inhibition. Unexpectedly, we demonstrate that activation of AMPK and constitutive mTORC1 signaling results in a synthetic lethal interaction across a range of AML primary samples and cell lines. The lack of constitutive mTORC1 activation in normal hematopoietic progenitors therefore suggests a therapeutic window for AMPK activation in the treatment of AML. Finally, we demonstrate that activation of the eIF2α/ATF4 signaling pathway is critical for the synthetic lethal interaction between activated mTORC1 and AMPK. Taken

Please cite this article in press as: Sujobert et al., Co-activation of AMPK and mTORC1 Induce Cytotoxicity in Acute Myeloid Leukemia, Cell Reports (2015), http://dx.doi.org/10.1016/j.celrep.2015.04.063

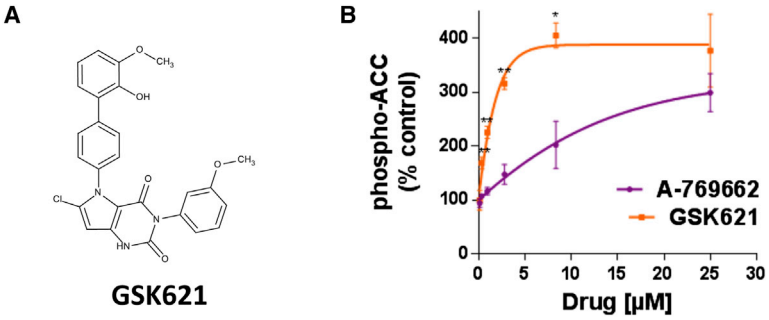

Figure 1. GSK621 Is a Specific and Potent AMPK Activator

(A) Chemical structure of GSK621.

(B) ACC (S79) phosphorylation, reflecting AMPK activation following increasing doses of GSK621 or A-769662 treatment, was assessed by ELISA in the human HEPG2 cell line. Results are presented for each condition as a percentage of vehicle-treated cells (n = 5).

(C) AML cell lines and primary AML cells from patient 2 were incubated 6 hr with vehicle or 30 μM GSK621, and protein extracts were immunoblotted for the indicated markers.

(D) Annexin 5 binding (bottom) and western blotting using AMPKα1 antibody (top) in MOLM-14 cells subjected to shRNA-induced AMPKα1 knockdown and cultured for 48 hr with vehicle or 30 μM GSK621 (n = 5).

(E) Trypan blue exclusion assay in single-cell cloned MOLM-14 cells transduced with a control (CTR) or a *PRKAA1* CRISPR and treated for 48 hr with vehicle or 30 μM GSK621. Right: western blotting in these cell lines using anti-AMPKα1 and anti-phospho-ACC (S79) antibodies. β-actin was used as a loading control in western blot experiments. Results in the graphs are expressed as the mean ± SEM. *p < 0.05, **p < 0.01, ***p < 0.001, ****p < 0.0001.

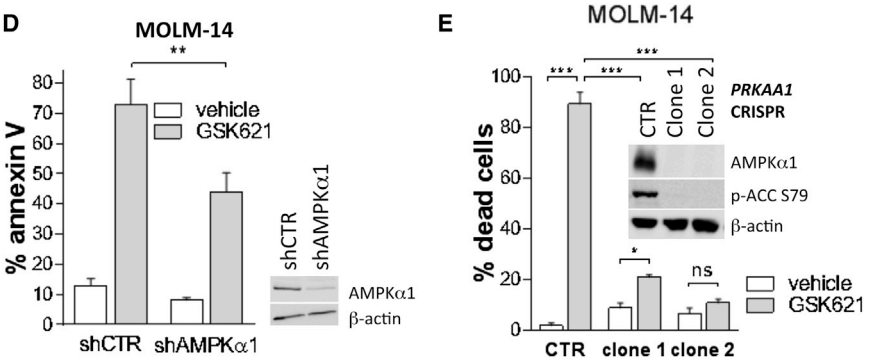

together, these data provide insights into the role of mTORC1 in AML and support the testing of therapeutic AMPK activators as a therapeutic strategy in cancers with mTORC1 activation.

RESULTS

AMPK Activation by GSK621

To directly and potently target AMPK, we developed a thienopyridone-derived compound GSK621 (Mirguet and Bouillot, 2011) (Figure 1A) that consistently activated AMPK recombinant heterotrimers in vitro, however, less potently that the tool compound A-769662 (Figure S1A). In cellular assays, GSK621 was at the opposite more potent than A-769662 at inducing AMPK activation, as measured by the level of ACC phosphorylation (Figure 1B). We hypothesize that differences in intracellular uptake may account for these results, as in MOLM-14 cells 200 μM A-769662 is barely as potent as 30 μM GSK621 at inducing ACC (S79) and ULK1 (S555) phosphorylation, two well-characterized direct AMPK substrates (Egan et al., 2011) (Figure S1B). In AML cell lines (MOLM-14, HL-60, and OCI-AML3) and primary AML samples, GSK621 markedly increased phosphorylation at AMPKα T172, a marker of AMPK activation, and also stimulated the phosphorylation of ACC (S79) and ULK1 (S555) (Figure 1C). These results suggest that GSK621 is a potent AMPK activator in AML cells.

To clarify whether these effects are dependent on AMPK in AML cells, we depleted MOLM-14 cells of AMPKα1, which is the only AMPK catalytic subunit isoform expressed in hematopoietic cells (Figures S1D and S1E). To that end, we first used lentivirally expressed anti-AMPKα1 small hairpin RNA (shRNA) in MOLM-14 cells. Following efficient AMPKα1 knockdown (Figure 1D), we incubated MOLM-14 cells with vehicle or GSK621. AMPKα1-depleted cells had reduced annexin V positivity after treatment with GSK621 (43.9% versus 73% for scrambled shRNA, p < 0.01; Figure 1D). To confirm these results, we deleted the *PRKAA1* gene that encodes AMPKα1 by CRISPR/Cas9 genome editing. MOLM-14 cells with homozygous *PRKAA1* deletion lose AMPK function (Figures 1E, right, and S1E) and were significantly protected from GSK621-induced cytotoxicity in contrast to cells expressing control CRISPR (Figure 1E, left). Moreover, prolonged exposure to GSK621 of a bulk lentivirally transduced population led to the gradual selection of MOLM-14 cells lacking AMPKα1 expression (Figure S1F), suggesting that AMPKα1 depletion protected AML cells from GSK621 cytotoxicity. We conclude

Table 1. Clinical and Molecular Characteristics of AML Patients

No.	Age (yr)	FAB	Cytogenetic	Molecular	GSK621	R
AML#1	69	AML5	46, XX, t(11;22)	$EVI1^{over}$	X	X
AML#2	65	AML5	46, XY	FLT3-ITD, $NPM1^{mut}$, $DNMT3A^{mut}$	X	
AML#3	78	AML5	46, XY	—	X	X
AML#4	75	AML1	46, XX	—	X	
AML#5	40	AML4	46, XX	FLT3-ITD, $NPM1^{mut}$	X	
AML#6	81	AML1	46, XX	FLT3-ITD, $NPM1^{mut}$, $DNMT3A^{mut}$	X	
AML#7	48	AML4	46, XY, del(9)	—	X	
AML#8	52	AML5	45, XX, −13, der(19)t(13;19)	—	X	
AML#9	68	AML1	46, XX	FLT3-ITD, $NPM1^{mut}$	X	
AML#10	77	AML1	46, XY	$IDH2^{mut}$, $ASXL1^{mut}$	X	
AML#11	61	AML5	46, XY	$SRSF2^{mut}$	X	
AML#12	76	AML1	46, XX	N/A	X	X
AML#13	74	sAML	46, XX, 5q-	—	X	X
AML#14	76	AML1	46 XX	$IDH2^{mut}$	X	X
AML#15	67	AML2	46 XX	FLT3-ITD	X	X
AML#16	68	sAML	46 XX	FLT3-ITD, $NPM1^{mut}$	X	X

FAB, French American British Classification of AML; sAML, secondary AML; $EVI1^{over}$, overexpression of *ecotropic virus integration site 1*; FLT3-ITD, *FLT3* Internal Tandem Duplication; $NPM1^{mut}$, *Nucleophosmin 1* mutation; $DNMT3A^{mut}$, *DNA (cytosine-5-)-methyltransferase 3 alpha* mutation; $IDH2^{mut}$, *Isocitrate Dehydrogenase 2* mutation; $ASXL1^{mut}$, *additional sex combs like 1* mutation; $SRSF2^{mut}$, *Serine/arginine-rich Splicing Factor 2* mutation; —, no molecular abnormality detected; N/A, information not available; R, rapamycin; X, sample involved in experiments done using GSK621 or rapamycin as indicated.

from these results that GSK621 is a specific AMPK agonist in AML cells.

GSK621 Selectively Kills AML Cells In Vitro and In Vivo

To determine the activity of GSK621 in AML, we assayed a set of 20 cell lines that captures the diversity of molecular abnormalities across this disease (Table S1). IC_{50} of GSK621 for each cell line ranged from 13 to 30 μM (Figures S2A and S2B). GSK621 (30 μM) reduced the proliferation of all 20 lines and increased apoptosis in 17 (85%) lines (Figure 2A; Figures S2C and S2D). We also exposed 16 primary AML samples corresponding to different AML subtypes (Table 1) to 30 μM GSK621 and consistently observed a significant induction of annexin V staining ($p < 0.01$ compared to vehicle treatment, Figure 2B). In contrast, the same concentration of GSK621 had no effect on annexin V positivity in normal human $CD34^+$ hematopoietic progenitor cells ($n = 9$, $p = 0.84$, Figure 2B).

To assess the impact of GSK621 on leukemic progenitor cells, we generated murine AMLs by transduction of bone marrow hematopoietic cells with either MLL-ENL (Barabé et al., 2007) or FLT3-ITD (Mizuki et al., 2000). After treatment with vehicle or 30 μM GSK621, AML cells were tested for serial replating capacity (Figure 2C), which is a well-established indicator of stemness in vitro (Yeung et al., 2010). GSK621 significantly reduced colony formation after each replating for both MLL-ENL and FLT3-ITD AMLs (Figure 2D), suggesting that GSK621 treatment depletes not only the bulk, but also the AML progenitor population in vitro.

Next, we determined GSK621 in vivo activity by xenografting MOLM-14 cells and treating with intraperitoneal injections of vehicle or GSK621. GSK621 (30 mg/kg twice daily) reduced leukemia growth (Figure 2E) and significantly extended survival compared to vehicle-treated animals or those treated with 10 mg/kg twice daily GSK621 (Figure 2F). These results correlated to enhanced AMPK activity (assessed by increased ACC S79 phosphorylation) and the induction of apoptosis (by TUNEL staining) (Figures 2G and S2E). As expected, GSK621 serum concentrations 5 hr after dosing were significantly higher in mice receiving 30 mg/kg compared to 10 mg/kg (Figure 2H). In GSK621-treated mice, no apparent toxicity was observed on hematopoiesis (Figure S2F), supporting the notion of a differential sensitivity to GSK621 between normal and leukemic cells.

AMPK Activation Induces Autophagy and Cell Death in AML

Although GSK621 clearly induced apoptosis across AML subtypes, we hypothesized that AMPK activation would also induce autophagy. As previously suggested, AMPK activation may promote autophagy to restore energy balance (Egan et al., 2011; Kim et al., 2011). Using transmission electronic microscopy, we observed that GSK621 induced the formation of numerous intracytoplasmic vacuoles including autophagosomes, as defined by double membrane vesicles with cytoplasmic material (Figure 3A).

mTORC1 is a well-documented inhibitor of autophagy (Lamb et al., 2013), but the effects of mTORC1 inhibition on autophagy depend on both cell type (Budovskaya et al., 2004; Mizushima et al., 2010; Takeuchi et al., 2005) and cellular context (Sheen et al., 2011). In MOLM-14 cells, rapamycin had no impact on autophagosome formation (Figure 3A). Similarly, rapamycin did not promote LC3B-II accumulation by western blotting in AML cell lines and primary AML samples, in contrast with GSK621 (Figure 3B). We confirmed autophagy induction in GSK621-treated

Please cite this article in press as: Sujobert et al., Co-activation of AMPK and mTORC1 Induce Cytotoxicity in Acute Myeloid Leukemia, Cell Reports (2015), http://dx.doi.org/10.1016/j.celrep.2015.04.063

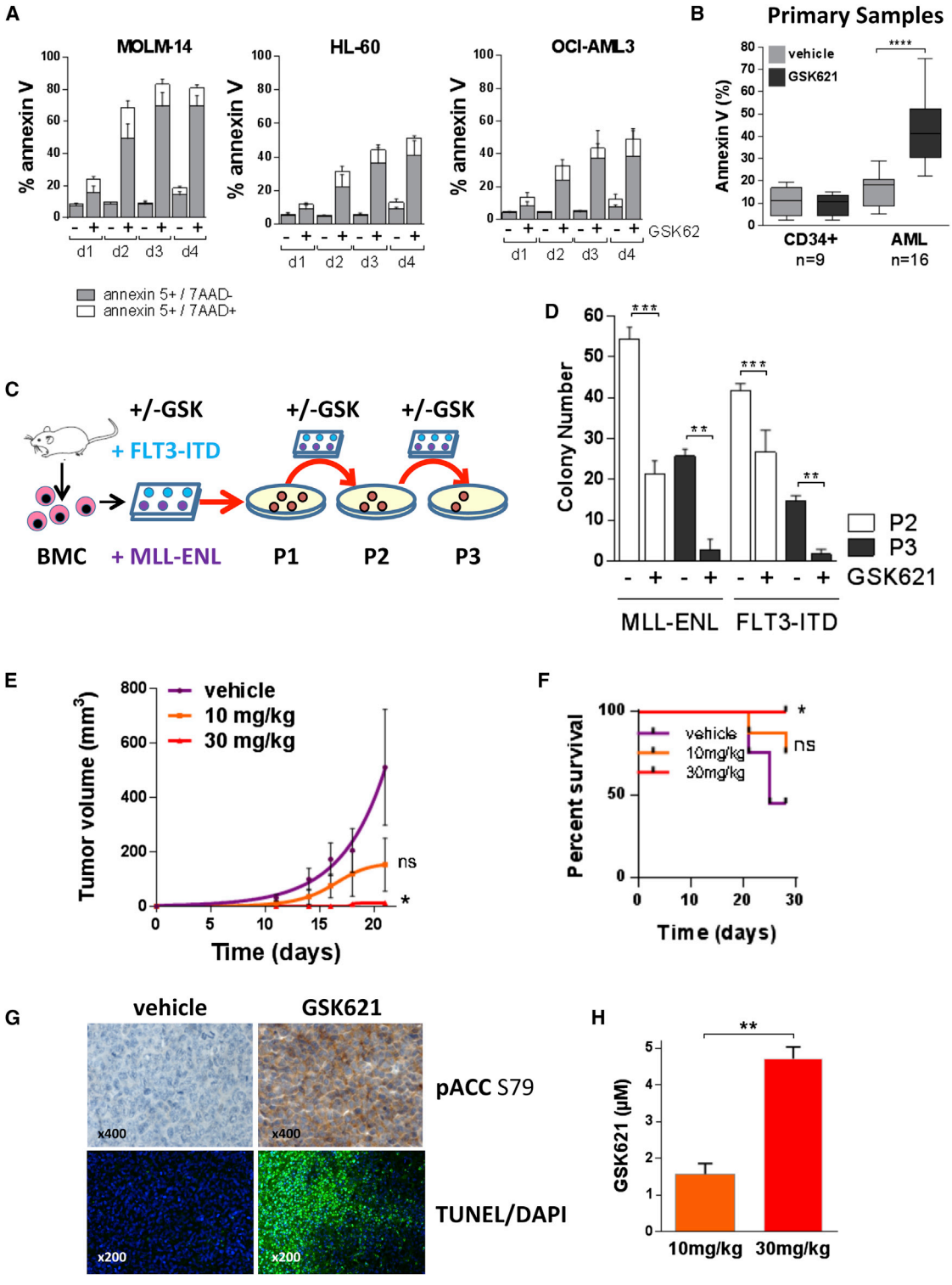

Figure 2. GSK621 Induces Anti-leukemic Activity in AML

(A) Apoptosis was determined in AML cell lines (MOLM-14, HL-60, OCI-AML3) incubated with vehicle or 30 μM GSK621 for up to 4 days by positivity for Annexin V and negativity for 7-AAD staining by flow cytometry.

(B) Primary normal hematopoietic CD34$^+$ progenitor cells (referred to as CD34$^+$) and cells from AML patients (AML) (CD34$^+$, n = 9; AML, n = 16) were cultured 48 hr with vehicle or 30 μM GSK621. Apoptosis was assessed by annexin V binding by flow cytometry.

(legend continued on next page)

cells by flow cytometry for monodansylcadaverin (MDC) (Vázquez and Colombo, 2009) (Figures 3C and 3D), and by immunofluorescence analysis of LC3B protein, which showed a shift from a diffuse intracellular localization to a dot-shaped distribution after GSK621 exposure (Figure 3E).

In MOLM-14 cells, chloroquine blocked the degradation of autophagosomes, as attested by increased LC3B-II accumulation (Figure 3F, top) (Mizushima et al., 2010). In the same chloroquine-treated AML cells, addition of GSK621 further induced LC3B-II expression, consistent with autophagy induction. In GSK621-treated MOLM-14 cells, chloroquine reduced annexin V staining, suggesting that autophagy inhibition protected AML cells from GSK621-induced cytotoxicity (Figure 3F, bottom). Autophagy related (ATG) 5 and 7 play a critical role in the formation of autophagosomes (Lamb et al., 2013). ATG7 knockdown reduced GSK621-induced autophagy, as assessed by western blotting in MOLM-14 cells (Figure 3G, top), and GSK621-induced apoptosis was reduced after knockdown of ATG7 (Figure 3G, bottom) or ATG5 (Figure S3). Knockdown of ATG7 rescued the loss of clonogenic growth capacity induced by GSK621 (Figure 3H). Together these results suggest that GSK621 treatment triggers autophagy, which partially contributes to AML cell death.

AMPK and mTORC1 Activation Are Synthetically Lethal in AML

We hypothesized two different models (Figure 4A) for the role of mTORC1 activity in the context of AMPK activation that may account for the preferential cytotoxicity of GSK621 in AML versus normal hematopoietic cells. In the first model (oncogene addiction), GSK621-induced AMPK activation suppresses mTORC1 activity, as we observed in HEK293 cells (Figure S4A) and previously shown after treatment of mouse embryonic fibroblasts (MEFs) with 5-aminoimidazole-4-carboxamide-1-β-D-ribofuranoside (AICAR) (Gwinn et al., 2008). In this model, inhibition of mTORC1 directly contributes to AML cell death. Arguing against this hypothesis, GSK621 did not inhibit mTORC1 in AML cell lines (MOLM-14, HL-60, and OCI-AML3) and primary AML samples (Figure 4B), based on persistent phosphorylation of the mTORC1 target p70S6K (T389). This indicates dissociation between AMPK activation and mTORC1 suppression in AML. Similar results were reported in glioma, suggesting that the classical axis connecting AMPK with mTORC1 axis is cell type dependent (Liu et al., 2014).

In the second model (synthetic lethality), sustained mTORC1 activity is required for the cytotoxic response to AMPK activation. To test this possibility, we first ectopically expressed a constitutively active AKT allele (myrAKT) (Kharas et al., 2010) in normal human CD34-positive ($CD34^+$) hematopoietic progenitors. myrAKT activated mTORC1 in these cells, as evidenced by phosphorylation of P70S6K (T389) and 4E-BP1 (S65) (Figure 4C, right). GSK621 induced apoptosis only in myrAKT-transduced $CD34^+$ cells and not in control cells (Figure 4C, left). Strikingly, this effect was reversed by co-treatment with rapamycin, indicating that mTORC1 activity is required for GSK621-induced cytotoxicity (Figure 4C, left). We overactivated mTORC1 in the MOLM-14 cell line by deleting the negative regulator *TSC2* (Inoki et al., 2002, 2003) by CRISPR/Cas9 genome editing (Figure 4D). Deletion of *TSC2* resulted in mTORC1 overactivation (based on increased p70S6K (T389) phosphorylation) and enhanced the cytotoxicity of GSK621 (Figure 4D).

Strikingly, inhibition of mTORC1 by shRNA knockdown of raptor or mTOR (Figures 4E and S4B) or by rapamycin (Figures 4F and S4C) protected AML cell lines from GSK621-induced apoptosis. We confirmed these results in primary AML samples in which rapamycin protected AML cells from apoptosis induced by GSK621 (Figure 4G). We also used two other direct AMPK activators, A769662 (Cool et al., 2006) and compound 991 (Xiao et al., 2013). In AML cell lines, 991 induced apoptosis and co-incubation with rapamycin significantly protected from 991 (Figure 4H). Cytotoxicity induced by A769662 was variable across AML cell lines, as reported (Green et al., 2010), with significant effects observed only in MOLM-14 cells (Figure 4H; data not shown in HL-60 and OCI-AML2). Co-treatment with rapamycin also protected MOLM-14 cells from A769662-induced cytotoxicity (Figure 4H). While GSK621 induced cytoplasmic vacuoles, pyknotic nuclei, and changes in cellular morphology in primary AML cells, co-treatment with rapamycin blocked these effects (Figure 4I). We conclude from these data that mTORC1 activity is critical for the cytotoxic effects observed upon treatment with AMPK activators including GSK621 in AML.

Synthetic Lethality between AMPK and mTORC1 Involves eIF2α/ATF4

To investigate the molecular basis of the synthetic lethal interaction between mTORC1 and AMPK, we generated an unbiased gene expression analysis in MOLM-14 cells treated with GSK621 or co-treated with GSK621 and rapamycin. Among the top ten Ingenuity canonical pathways scored by this analysis (Figure S5A), the unfolded protein response (UPR) was the most significantly inhibited by the addition of rapamycin in GSK621-treated MOLM-14 cells (Figure 5A, –log(p value) = 6.28). In fact, GSK621 induced eiF2α phosphorylation—a hallmark of UPR activation—as well as upregulation of terminal effectors of

(C) Schematic representation of the mouse leukemia cell methylcellulose experiments. BMC, mouse bone marrow cells; GSK, GSK621; P2, second methylcellulosis plating; P3, third methylcellulosis plating.

(D) Cells were plated at 5×10^4/ml in methylcellulose and incubated with vehicle or 30 μM GSK621. Colony formation was assessed at day 7. At the end of methylcellulose culture, cells were washed in PBS seeded again in methylcellulose with or without GSK621 (this step is referred to as first replating). Up to three successive replatings were performed.

(E and F) Tumor growth and survival (Kaplan-Meier curve) in MOLM-14 cells xenografted into nude mice treated with vehicle, 10 mg/kg, or 30 mg/kg GSK621 by twice-daily intraperitoneal injections.

(G) Tumor sections were stained by TUNEL and DAPI or labeled with an anti-phospho-ACC (S79) antibody. Representative images of three experiments are shown.

(H) Plasma concentrations of GSK621 in mice treated with 10 or 30 mg/kg GSK621 5 hr after intraperitoneal injection (n = 3 for each). Results in the graphs are expressed as the mean ± SEM. *$p < 0.05$, **$p < 0.01$.

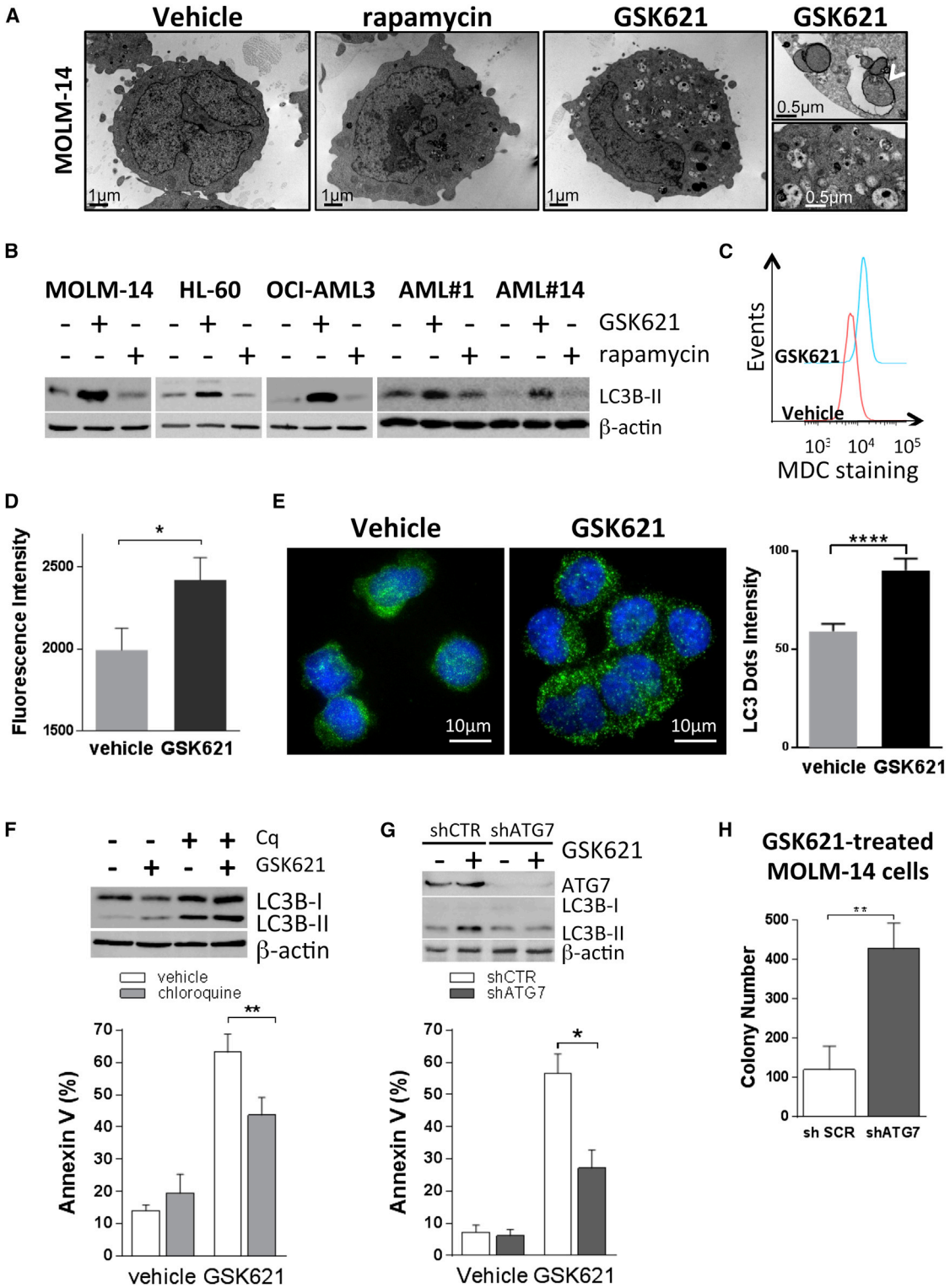

Figure 3. Autophagy Is a Trigger of GSK621-Induced AML Cell Death

(A) Electron microscopy-captured images of MOLM-14 cells treated 24 hr with vehicle, 10 nM rapamycin, or 30 µM GSK621 (12,000× magnification). Details of GSK621-treated MOLM-14 cells (24,000× magnifications) are provided, and the white arrowhead indicates the double membrane feature characteristic of autophagy.

(legend continued on next page)

the eiF2α pathway (ATF4, CHOP) (Clarke et al., 2014) in MOLM-14 and primary AML cells (Figures 5B and S5B). GSK621 treatment also induced PERK phosphorylation, a marker of ER stress, in AML cells (Figure S5C). By contrast, GSK621 did not induce eIF2α phosphorylation in normal $CD34^+$ hematopoietic progenitor cells (Figure S5D) or in MEFs lacking AMPKα1 and AMPKα2 expression (Figure S5E) (Laderoute et al., 2006), supporting the notion that eIF2α was a consequence of GSK621-induced AMPK activation in AML cells.

We followed mRNA expression of the main effectors of the eIF2α pathway—*ATF4*, *ATG12*, and *CHOP*—in MOLM-14 cells. We observed that while GSK621 enhanced their expression compared to vehicle-treated cells, *ATF4*, *ATG12*, and *CHOP* mRNA remained at steady-state in AML cells co-treated with rapamycin and GSK621 (Figure 5C). In fact, the level of ATF4 protein increased with mTORC1 activity induced by *TSC2* ablation and decreased with mTORC1 inhibition by rapamycin treatment in MOLM-14 cells (Figure 5D). These results suggest that mTORC1 is required for the full activation of eIF2α pathway upon GSK621 treatment.

To further understand the contribution of the eIF2α pathway to GSK621-induced cytotoxicity, we first ectopically expressed an inactive *EIF2A* S52A mutant (Harding et al., 2009) in MOLM-14 cells. Cells expressing *EIF2A* S52A had reduced GSK621-induced ATF4 expression and were partially protected from GSK621-induced cytotoxicity (Figure S5F). We inhibited the UPR pathway with phenylbutyric acid (PBA) (Ozcan et al., 2006) or a PERK inhibitor (GSK2656157 compound (Atkins et al., 2013) in MOLM-14 cells and observed that co-incubation with these compounds significantly protected from GSK621-induced cytotoxicity (Figures S5G and S5H). Next, we used pharmacological and genetic approaches to overactivate eIF2α signaling pathway in MOLM-14 cells. Thapsigargin is an ER calcium ATPase inhibitor that activates the eIF2α/ATF4 pathway (van Galen et al., 2014). In MOLM-14 cells, co-incubation with thapsigargin or ectopic overexpression of ATF4 abrogated the protective effect of rapamycin on GSK621-induced cytotoxicity (Figures 5E and 5F). These data indicate that the eIF2α/ATF4 pathway is involved in the synthetic lethality between AMPK and mTORC1 co-activation in AML.

DISCUSSION

AMPK is a central regulator of energy balance in mammalian cells. Several groups have previously demonstrated its importance in normal hematopoietic stem cell homeostasis (Gan et al., 2010; Gurumurthy et al., 2010; Nakada et al., 2010). Here, we showed that specific pharmacological AMPK activation suppresses tumor growth in AML. GSK621 exerted significant anti-leukemic activity against AML cell lines in vitro and in vivo, as well as primary human AML samples. Strikingly, GSK621 targets leukemic progenitor cells but spares normal human hematopoietic progenitor cells, highlighting the importance of AMPK in transformed cells and suggesting a promising therapeutic opportunity for AMPK activation in AML.

Among mechanisms underlying cytotoxicity downstream of GSK621 treatment, we observed both apoptosis and autophagy. Autophagy is generally enhanced by AMPK activation in parallel with other energy-sparing processes (Egan et al., 2011; Kim et al., 2011; Sheen et al., 2011) and has been implicated in chemotherapy resistance (Sui et al., 2013) and cell survival after oncogenic stress (Elgendy et al., 2011). In contrast, we found that GSK621 treatment led to autophagic cell death in AML. mTORC1 is the essential negative regulator of nutrient starvation-induced autophagy (Levine and Kroemer, 2008) and AMPK inhibition contributes to autophagy-mediated cell survival in this context (Kim et al., 2011). In AML, we found that specific mTORC1 inhibition did not promote autophagy, in contrast to most currently described models (Kim et al., 2011). We also observed a dissociation between AMPK activation and mTORC1 inhibition, as recently reported in glioma cells (Liu et al., 2014). As such, GSK621 induces mTORC1-independent autophagy downstream of AMPK.

To date, no evidence of oncogenic addiction to mTORC1 has been observed in AML, despite the finding of constitutive mTORC1 activity in this disease (Tamburini et al., 2009). Furthermore, despite the prevailing view of mTORC1 as a target for pharmacological inhibition in cancer (Kelsey and Manning, 2013), clinical trials of mTORC1 inhibitors such as rapamycin have failed to demonstrate broad activity in AML (Amadori et al., 2012; Perl et al., 2009). Here, we propose a model in which mTORC1 and AMPK contribute to a unique, synthetic lethal interaction in AML. Sustained mTORC1 activation in AML was required for cytotoxicity induced by activated AMPK. This cytotoxicity could be abrogated pharmacologically by rapamycin or amplified by mTORC1 overactivation driven by *TSC2* loss. In normal hematopoietic progenitors, low mTORC1 activity and/or coupled AMPK and mTORC1 activities (Figure S5D)—which is in contrast to the observations made in AML—can explain the limited toxicity of GSK621 treatment. Indeed, synthetic

(B) Western blotting of MOLM-14, HL-60, OCI-AML3 AML cell lines and primary AML samples (AML#1 and AML#14) treated 24 hr with 30 μM GSK621 or 10 nM rapamycin using anti-LC3B antibody.

(C and D) Flow cytometry analysis of monodansylcadaverin (MDC) staining of vehicle- or GSK621 (30 μM)-treated MOLM-14 cells (C: representative histograms and D: fluorescence intensity quantification, n = 6).

(E) Immunofluorescence analysis using an anti-LC3B antibody (left) and quantification of LC3B dots signal intensity (right) in vehicle- or GSK621-treated (30 μM) MOLM-14 cells.

(F) MOLM-14 cells were cultured 48 hr with vehicle, 30 μM GSK621, 10 μM chloroquine, or combination. Top: western blotting using LC3-B antibody; bottom: annexin V staining experiments (n = 5).

(G) ATG7 knockdown was induced in MOLM-14 cells, which were then treated with vehicle or 30 μM GSK621 for 48 hr. Bottom: flow cytometry analysis of annexin V binding (n = 3). Top: western blotting with ATG7 and LC3B antibodies.

(H) Colony formation in MOLM-14 cells lentivirally transduced with scramble or ATG7 shRNA. Cells were incubated for 48 hr with vehicle or 30 μM GSK621 and then cultured in methylcellulose for 7 days. β-actin is used as a control for loading. Results in the graphs are expressed as the mean ± SEM. *$p < 0.05$, **$p < 0.01$, ***$p > 0.001$, ****$p < 0.0001$.

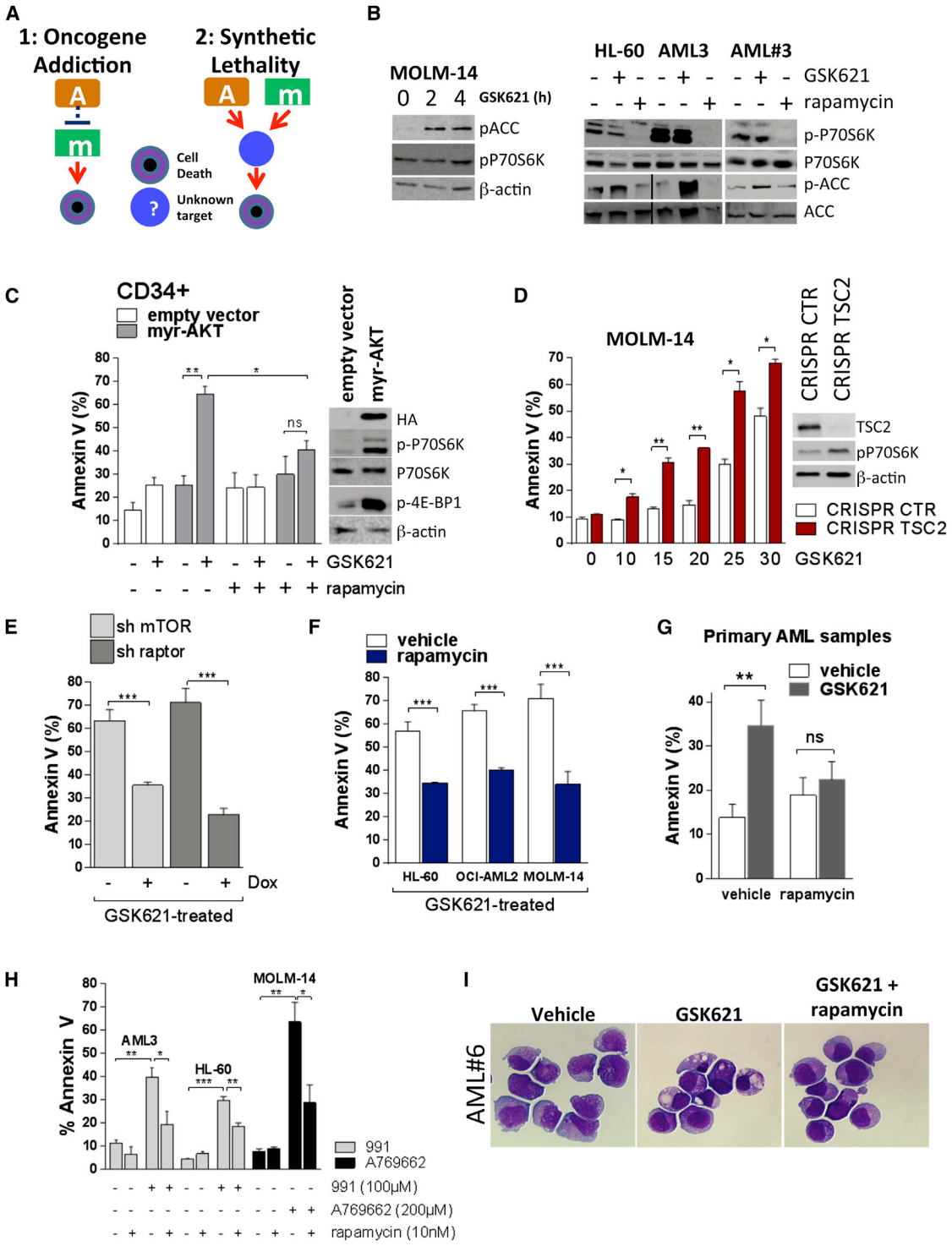

Figure 4. AMPK and mTORC1 Co-activation Is Synthetically Lethal in AML

(A) Schematic representation of the oncogene addiction (1) and synthetic lethal (2) hypothesis concerning the role of mTORC1 upon AMPK activation.

(B) Western blotting in MOLM-14 cells treated during 2 or 4 hr with 30 μM GSK621 (left) or in HL-60 and OCI-AML3 cell lines and primary sample AML#3 treated 6 hr with vehicle, 10 nM rapamycin, or 30 μM GSK621 (right) using anti-phospho-ACC (S79), -phospho-p70S6K (T389), -ACC, and -P70S6K antibodies.

(C) Right: western blotting of human $CD34^+$ hematopoietic progenitors (referred to as "$CD34^+$ cells") lentivirally transduced with empty vector or with a HA-tagged myrAKT construct. Left: flow cytometry determination of Annexin V binding in $CD34^+$ cells lentivirally transduced with empty vector or with a myrAKT construct and treated with vehicle or 10 nM rapamycin for 24 hr followed by addition of either vehicle or 100 μM GSK621 for 48 hr (n = 3).

(legend continued on next page)

lethality observed with AMPK activation can be induced solely by myr-AKT-driven mTORC1 activation in these cells. The magnitude of mTORC1 activity thus determines the impact of AMPK activation and therefore the specific cytotoxicity of GSK621.

From an unbiased analysis, we found that co-activation of the eIF2α/ATF4 pathway by both mTORC1 and AMPK was associated with the selective cytotoxicity of GSK621 on AML cells versus normal hematopoietic cells. In fact, Ozcan and colleagues previously showed that mTORC1 overactivation resulting from tuberous sclerosis complex (TSC1 or TSC2) disruption triggers the unfold protein response, which includes eIF2α activation (Ozcan et al., 2008). Recent work showed that transcriptional regulation of ATF4 by mTORC1 involves the *trans*-activating function of c-MYC (Babcock et al., 2013). In AML, we showed that mTORC1 activation promoted ATF4 accumulation and that overexpression of ATF4 abrogated protection from GSK621 cytotoxicity induced by rapamycin in leukemic cells. Together these results suggest that the eIF2α/ATF4 signaling pathway coordinate signals resulting from AMPK and mTORC1 co-activation leading to AML cell death.

These data demonstrate an unexpected role of mTORC1 in the cytotoxic response to metabolic stress and provide the biologic rationale for testing AMPK activators in clinical trials in AML and other cancers with constitutive mTORC1 signaling.

EXPERIMENTAL PROCEDURES

Full details are provided in the Supplemental Experimental Procedures.

Human Primary Samples

Patients and healthy donors provided a written informed consent in accordance with the declaration of Helsinki. The characteristics of AML patients are provided in Table 1.

Cell Lines

Characteristics of cell lines used are provided in Table S1.

Reagents and Constructs

Rapamycin, chloroquine, oligomycin, puromycin, monodansylcadaverin (MDC), thapsigargin, and doxycycline (Dox) were from Sigma-Aldrich (Sigma-Aldrich). A769662 was form Santa Cruz Biotechnology. The 991 compound was synthesized by GlaxoSmithKline Research Center, as reported (Xiao et al., 2013). We utilized myrAKT and ATF4 plasmids from Addgene (number 31790 and 26114, respectively) (Calvisi et al., 2011; Wang et al., 2009) that were cloned using the Gateway system (Life Technologies) in pLenti PGK Blasti DEST or in pLenti PGK Puro DEST (Addgene plasmids 19068 and 17451, respectively) (Campeau et al., 2009).

RNA Interference

PLKO and Tet-pLKO-puro plasmids (Addgene plasmids 8453 and 21915, respectively (Stewart et al., 2003; Wiederschain et al., 2009)) and pTRIPZ plasmid (Thermo Scientific) were used to generate lentivirus able to stably deliver constitutive or doxycycline-inducible hairpins to AML cell lines.

CRISPR/Cas9 Genome Editing

We cloned small guide RNA (sgRNA) guides targeting by using the Optimized Crispr Design application from Dr. F. Zhang's lab (http://crispr.mit.edu/) into the lentiCRISPR plasmid (Addgene plasmid 49535).

Monodansylcadaverine

Cells were incubated 0.5 hr at 37°C with 5 μM monodansylcadaverin and then washed three times and analyzed on a LSRII cytometer (excitation and emission wavelength 353 and 512 nm, respectively).

AML Xenografts in NUDE Mice

All experiments were conducted in accordance with the guidelines of the Association for Assessment and Accreditation of Laboratory Animal Care International and after approval of the local ethics committee.

Mice Leukemic Cells Clonogenic Assay

Colony formation was assayed in bone marrow cells from C57B6 mice transduced with MLL-ENL or FLT3-ITD oncogenes. After 1 week of culture with 10 ng/ml interleukin 6 (IL-6) and 50 ng/ml SCF (Peprotech), 5×10^4 cells were plated in Methocult medium with vehicle or 30 μmol/l GSK621. Colonies were numbered at 7 days.

Transmission Electron Microscopy

AML cells (10^6) were fixed and then dehydrated by successive ethanol washes (70%, 90%, 100%, and 100%) and impregnated with epoxy resin. Sections (80–90 nm) were prepared using a Reichert Ultracut S ultramicrotome, stained with 2% uranyl acetate plus Reynold's lead citrate, and visualized under a JEOL 1011 transmission electron microscope with a GATAN Erlangshen charge-coupled device (CCD) camera.

Immunofluorescence

MOLM-14 cells (2×10^5) were fixed in methanol after cytocentrifugation, washed in PBS, and blocked in 3% BSA PBS. Cells were incubated 1 hr with anti-LC3 antibody and then with GFP-coupled anti-rabbit antibody. Analysis was done on a Zeiss inverted microscope, and spots were automatically quantified with the open-source software CellProfiler (Kamentsky et al., 2011) with the Enhance Features and Identify Primary Objects modules.

qPCR

qPCR was then performed on a Lightcycler 480 (Roche). Primers sequences are provided in the Supplemental Experimental Procedures.

Gene Expression Profiling

cDNA were hybridized on GeneChip Human Gene MoGene-2_0-st from Affymetrix GeneChips. To find differentially expressed genes, we applied a classical ANOVA for each gene and made pairwise Tukey's post hoc tests between

(D) Left: annexin V binding in MOLM-14 cells lentivirally transduced with nontarget (CTR) or TSC2 sgRNA and treated with a dose range of GSK621 for 48 hr (n = 3). Right: western blotting of CTR or TSC2 sgRNA-expressing MOLM-14 cells.
(E) Annexin V binding in MOLM-14 cells transduced with doxycycline-inducible mTOR or raptor shRNA treated with 200 ng/ml doxycycline (Dox) for 4 days and then vehicle or 30 μM GSK621 was added (n = 3).
(F) Annexin V binding in AML cell lines treated with vehicle or 10 nM rapamycin for 24 hr and then vehicle or 30 μM GSK621 for 48 hr (n = 4).
(G) Primary AML samples were treated with vehicle or 10 nM rapamycin for 24 hr, and then vehicle or 30 μM GSK621 was added. Apoptosis was measured 48 hr later by annexin V binding (n = 7).
(H) Annexin V binding in AML cell lines treated with vehicle or 10 nM rapamycin for 24 hr and then vehicle or 100 μM 991 and vehicle or 200 μM A769662 for 48 hr (n = 3).
(I) May-Grünwald Giemsa (MGG) coloration of cytospin from a primary AML sample AML#6 treated with vehicle, 30 μM GSK621, or with 10 nM rapamycin and 30 μM GSK621. β-actin is used as a control for loading. Results in the graphs are expressed as the mean ± SEM. *$p < 0.05$, **$p < 0.01$, ***$p > 0.001$.

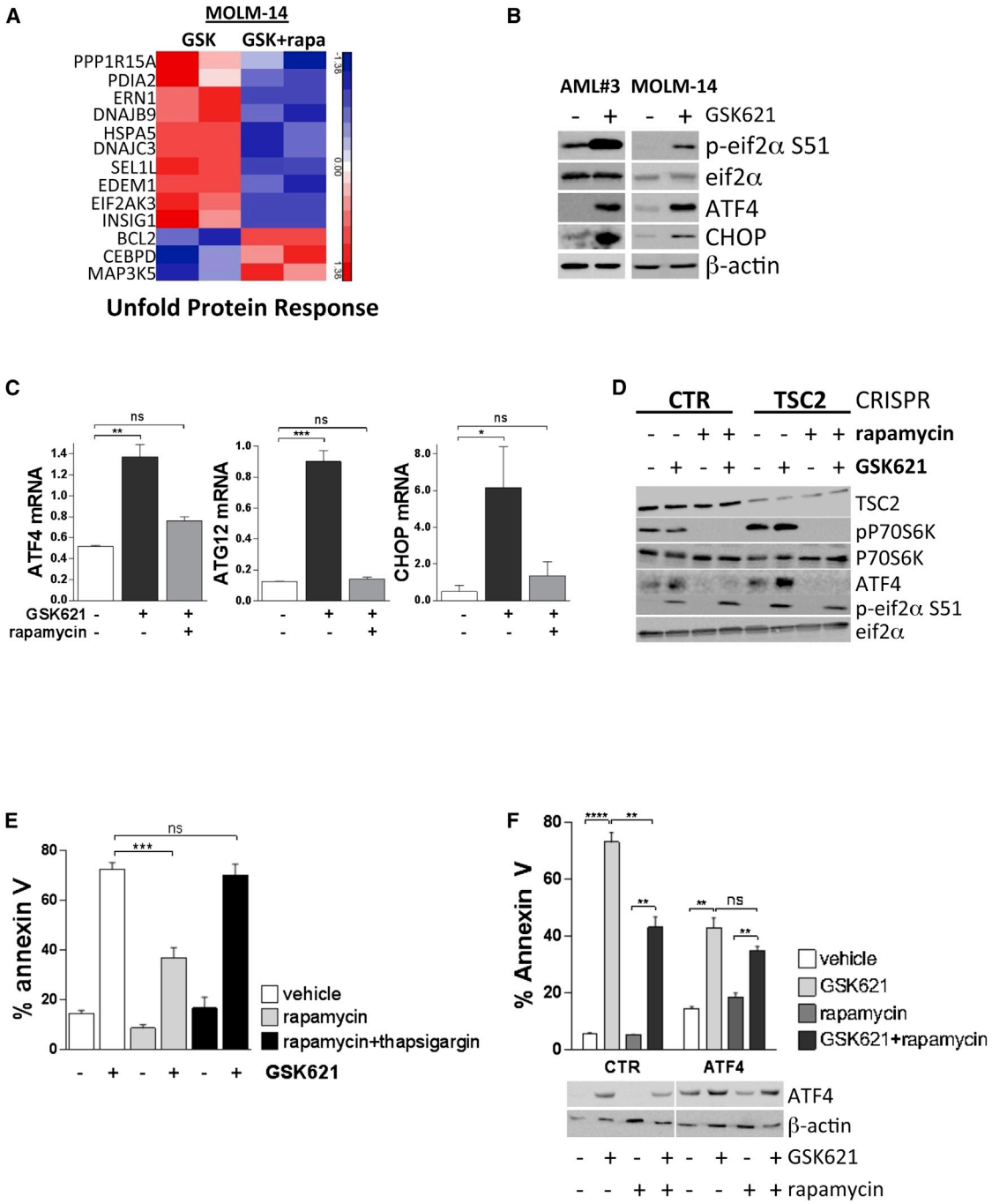

Figure 5. Synthetic Lethality between AMPK and mTORC1 Involves eIF2α/ATF4

(A) Heatmap representing the gene expression variations of 13 genes involved in the unfold protein response pathway. MOLM-14 cells were treated 24 hr with vehicle or 10 nM rapamycin and then exposed 12 hr to 30 μM GSK621.

(B) Western blotting in a primary AML sample (AML#3) and in the MOLM-14 cell line treated with vehicle or 30 μM GSK621 for 24 hr using anti-phospho-eIF2α (S51), anti-eIF2α, -ATF4, and -CHOP antibodies.

(C) Quantification by qPCR of *ATF4*, *ATG12*, and *CHOP* mRNA (normalized to *GAPDH* and *UBC*) in MOLM-14 cells treated with vehicle or 10 nM rapamycin for 24 hr and then vehicle or 30 μM GSK621 for 24 hr (n = 3).

(D) MOLM-14 cells were lentivirally transduced with a control (CTR) or a TSC2 CRISPR guide. Both CTR and TSC2 cell lines were treated with vehicle or 10 nM rapamycin during 24 hr and then incubated 6 hr with vehicle or 30 μM GSK621. Anti-phospho-P70S6K (T389), anti-P70S6K, anti-TSC2, anti-ATF4, anti-peIF2α (S51), and anti-eIF2α antibodies were used for western blotting.

(legend continued on next page)

groups. Then, we used p values and fold changes to filter and select differentially expressed genes with the Ingenuity Pathway Analysis software.

Statistics

Differences between the mean values obtained for the experimental groups were analyzed using the two-tailed Student's t test. Statistical analyses were performed using Prism software (GraphPad).

SUPPLEMENTAL INFORMATION

Supplemental Information includes Supplemental Experimental Procedures, five figures, and two tables and can be found with this article online at http://dx.doi.org/10.1016/j.celrep.2015.04.063.

AUTHOR CONTRIBUTIONS

P.S. designed and performed research analyzed data and wrote the manuscript. L.P. contributed to in vitro experiments design, performed experiments in primary samples (both AML and $CD34^+$), contributed to CRISPR experiments, and analyzed data. E.P. and F.Z. performed in vivo studies and analyzed data. A.G., M.L., E.C.T., J.-M.B., and E.N. performed experiments and analyzed data. J.D., I.N., A.S.G., J.M., M.-A.H., N.J., A.C., and T.A.D. performed experiments. O.H., M.F., B.V., C.L., and P.M. analyzed data. D.M.W., I.C.M., and D.B. analyzed data and wrote the manuscript. J.T. designed and supervised research program, analyzed data, and wrote the manuscript. All authors approved the final version of the manuscript.

ACKNOWLEDGMENTS

The authors would like to thank Olivier Mirguet and Anne Bouillot for the discovery and synthesis of GSK621, Véronique Bénéton for quantification of GSK621 levels in mouse sera, Pascal Grondin and Alizon Riou-Aymard for the in vitro AMPK screen assay (GSK Les Ulis). We also thank Alain Schmitt (Genomic Facility, Cochin Institute) for help with electron microscopy experiments and analysis, Franck Letourneur and Florent Dumont (transcriptomic Facility, Cochin Institute) for transcriptomic and bioinformatics analysis and Dr. Diane Damotte for helping in immunohistochemistry analysis. The authors also thank Dr. Bob Weinberg and Dr. Dmitri Wiederschain for sharing the pLKO and Tet-pLKO-puro plasmids, respectively, Dr. Eric Campeau for sharing pLenti PGK Puro DEST (w529-2) and pLenti PGK Blati DEST plasmids, Dr. Feng Zhang for sharing the lentiCRISPR plasmid, Dr. Xin Chen for the myrAKT plasmid, and Dr. Yihong Ye for the ATF4 plasmid, all through Addgene. We are also grateful to Dr. Nabih Azar (Pitie-Salpetriere Hospital, Paris, France) for contributing to the normal $CD34^+$ cell samples and to Dr. Isabelle Dusanter for providing human cord blood cells. P.S. was supported by grants from the INSERM (poste d'accueil INSERM) and from Association pour la Recherche sur le Cancer (ARC). A.G. received grants from Fondation pour la Recherche Medicale (FRM). J.-M.B. and E.N. are employees of the GlaxoSmithKline French research center (Les Ulis). D.M.W. is a paid consultant and receives research support from Novartis. He is also participating in an advisory board for Roche.

Received: December 26, 2014
Revised: March 20, 2015
Accepted: April 30, 2015
Published: May 21, 2015

REFERENCES

Amadori, S., Stasi, R., Martelli, A.M., Venditti, A., Meloni, G., Pane, F., Martinelli, G., Lunghi, M., Pagano, L., Cilloni, D., et al. (2012). Temsirolimus, an mTOR inhibitor, in combination with lower-dose clofarabine as salvage therapy for older patients with acute myeloid leukaemia: results of a phase II GIMEMA study (AML-1107). Br. J. Haematol. *156*, 205–212.

Atkins, C., Liu, Q., Minthorn, E., Zhang, S.Y., Figueroa, D.J., Moss, K., Stanley, T.B., Sanders, B., Goetz, A., Gaul, N., et al. (2013). Characterization of a novel PERK kinase inhibitor with antitumor and antiangiogenic activity. Cancer Res. *73*, 1993–2002.

Babcock, J.T., Nguyen, H.B., He, Y., Hendricks, J.W., Wek, R.C., and Quilliam, L.A. (2013). Mammalian target of rapamycin complex 1 (mTORC1) enhances bortezomib-induced death in tuberous sclerosis complex (TSC)-null cells by a c-MYC-dependent induction of the unfolded protein response. J. Biol. Chem. *288*, 15687–15698.

Barabé, F., Kennedy, J.A., Hope, K.J., and Dick, J.E. (2007). Modeling the initiation and progression of human acute leukemia in mice. Science *316*, 600–604.

Büchner, T., Schlenk, R.F., Schaich, M., Döhner, K., Krahl, R., Krauter, J., Heil, G., Krug, U., Sauerland, M.C., Heinecke, A., et al. (2012). Acute Myeloid Leukemia (AML): different treatment strategies versus a common standard arm—combined prospective analysis by the German AML Intergroup. J. Clin. Oncol. *30*, 3604–3610.

Budovskaya, Y.V., Stephan, J.S., Reggiori, F., Klionsky, D.J., and Herman, P.K. (2004). The Ras/cAMP-dependent protein kinase signaling pathway regulates an early step of the autophagy process in Saccharomyces cerevisiae. J. Biol. Chem. *279*, 20663–20671.

Calvisi, D.F., Wang, C., Ho, C., Ladu, S., Lee, S.A., Mattu, S., Destefanis, G., Delogu, S., Zimmermann, A., Ericsson, J., et al. (2011). Increased lipogenesis, induced by AKT-mTORC1-RPS6 signaling, promotes development of human hepatocellular carcinoma. Gastroenterology *140*, 1071–1083.

Campeau, E., Ruhl, V.E., Rodier, F., Smith, C.L., Rahmberg, B.L., Fuss, J.O., Campisi, J., Yaswen, P., Cooper, P.K., and Kaufman, P.D. (2009). A versatile viral system for expression and depletion of proteins in mammalian cells. PLoS ONE *4*, e6529.

Clarke, H.J., Chambers, J.E., Liniker, E., and Marciniak, S.J. (2014). Endoplasmic reticulum stress in malignancy. Cancer Cell *25*, 563–573.

Cool, B., Zinker, B., Chiou, W., Kifle, L., Cao, N., Perham, M., Dickinson, R., Adler, A., Gagne, G., Iyengar, R., et al. (2006). Identification and characterization of a small molecule AMPK activator that treats key components of type 2 diabetes and the metabolic syndrome. Cell Metab. *3*, 403–416.

Egan, D.F., Shackelford, D.B., Mihaylova, M.M., Gelino, S., Kohnz, R.A., Mair, W., Vasquez, D.S., Joshi, A., Gwinn, D.M., Taylor, R., et al. (2011). Phosphorylation of ULK1 (hATG1) by AMP-activated protein kinase connects energy sensing to mitophagy. Science *331*, 456–461.

Elgendy, M., Sheridan, C., Brumatti, G., and Martin, S.J. (2011). Oncogenic Ras-induced expression of Noxa and Beclin-1 promotes autophagic cell death and limits clonogenic survival. Mol. Cell *42*, 23–35.

Faubert, B., Boily, G., Izreig, S., Griss, T., Samborska, B., Dong, Z., Dupuy, F., Chambers, C., Fuerth, B.J., Viollet, B., et al. (2013). AMPK is a negative regulator of the Warburg effect and suppresses tumor growth in vivo. Cell Metab. *17*, 113–124.

Fullerton, M.D., Galic, S., Marcinko, K., Sikkema, S., Pulinilkunnil, T., Chen, Z.P., O'Neill, H.M., Ford, R.J., Palanivel, R., O'Brien, M., et al. (2013). Single phosphorylation sites in Acc1 and Acc2 regulate lipid homeostasis and the insulin-sensitizing effects of metformin. Nat. Med. *19*, 1649–1654.

Gan, B., Hu, J., Jiang, S., Liu, Y., Sahin, E., Zhuang, L., Fletcher-Sananikone, E., Colla, S., Wang, Y.A., Chin, L., and Depinho, R.A. (2010). Lkb1 regulates quiescence and metabolic homeostasis of haematopoietic stem cells. Nature *468*, 701–704.

(E) MOLM-14 cells were cultured 24 hr with vehicle, 10 nM rapamycin, or combination of 10 nM rapamycin and 5 nM thapsigargin. Vehicle or GSK621 (30 μM) was then added for an additional 48 hr, and annexin V staining was measured.

(F) *ATF4* was ectopically expressed in MOLM-14 cells using lentivirus. Cells were incubated 24 hr with vehicle or 10 nM rapamycin and then treated 48 hr with 30 μM GSK621. Top: annexin V staining. Bottom: western blotting using anti-ATF4 and anti-β-actin antibodies; CTR, control vector; ATF4, ATF4-expressing vector. Results in the graphs are expressed as the mean ± SEM. *$p < 0.05$, **$p < 0.01$, ***$p < 0.001$. ns, non-significant.

Please cite this article in press as: Sujobert et al., Co-activation of AMPK and mTORC1 Induce Cytotoxicity in Acute Myeloid Leukemia, Cell Reports (2015), http://dx.doi.org/10.1016/j.celrep.2015.04.063

Green, A.S., Chapuis, N., Maciel, T.T., Willems, L., Lambert, M., Arnoult, C., Boyer, O., Bardet, V., Park, S., Foretz, M., et al. (2010). The LKB1/AMPK signaling pathway has tumor suppressor activity in acute myeloid leukemia through the repression of mTOR-dependent oncogenic mRNA translation. Blood *116*, 4262–4273.

Gurumurthy, S., Xie, S.Z., Alagesan, B., Kim, J., Yusuf, R.Z., Saez, B., Tzatsos, A., Ozsolak, F., Milos, P., Ferrari, F., et al. (2010). The Lkb1 metabolic sensor maintains haematopoietic stem cell survival. Nature *468*, 659–663.

Gwinn, D.M., Shackelford, D.B., Egan, D.F., Mihaylova, M.M., Mery, A., Vasquez, D.S., Turk, B.E., and Shaw, R.J. (2008). AMPK phosphorylation of raptor mediates a metabolic checkpoint. Mol. Cell *30*, 214–226.

Hardie, D.G., Ross, F.A., and Hawley, S.A. (2012). AMPK: a nutrient and energy sensor that maintains energy homeostasis. Nat. Rev. Mol. Cell Biol. *13*, 251–262.

Harding, H.P., Zhang, Y., Scheuner, D., Chen, J.J., Kaufman, R.J., and Ron, D. (2009). Ppp1r15 gene knockout reveals an essential role for translation initiation factor 2 alpha (eIF2alpha) dephosphorylation in mammalian development. Proc. Natl. Acad. Sci. USA *106*, 1832–1837.

Inoki, K., Li, Y., Zhu, T., Wu, J., and Guan, K.L. (2002). TSC2 is phosphorylated and inhibited by Akt and suppresses mTOR signalling. Nat. Cell Biol. *4*, 648–657.

Inoki, K., Zhu, T., and Guan, K.L. (2003). TSC2 mediates cellular energy response to control cell growth and survival. Cell *115*, 577–590.

Jeon, S.M., Chandel, N.S., and Hay, N. (2012). AMPK regulates NADPH homeostasis to promote tumour cell survival during energy stress. Nature *485*, 661–665.

Kamentsky, L., Jones, T.R., Fraser, A., Bray, M.A., Logan, D.J., Madden, K.L., Ljosa, V., Rueden, C., Eliceiri, K.W., and Carpenter, A.E. (2011). Improved structure, function and compatibility for CellProfiler: modular high-throughput image analysis software. Bioinformatics *27*, 1179–1180.

Kelsey, I., and Manning, B.D. (2013). mTORC1 status dictates tumor response to targeted therapeutics. Sci. Signal. *6*, pe31.

Kharas, M.G., Okabe, R., Ganis, J.J., Gozo, M., Khandan, T., Paktinat, M., Gilliland, D.G., and Gritsman, K. (2010). Constitutively active AKT depletes hematopoietic stem cells and induces leukemia in mice. Blood *115*, 1406–1415.

Kim, J., Kundu, M., Viollet, B., and Guan, K.L. (2011). AMPK and mTOR regulate autophagy through direct phosphorylation of Ulk1. Nat. Cell Biol. *13*, 132–141.

Laderoute, K.R., Amin, K., Calaoagan, J.M., Knapp, M., Le, T., Orduna, J., Foretz, M., and Viollet, B. (2006). 5′-AMP-activated protein kinase (AMPK) is induced by low-oxygen and glucose deprivation conditions found in solid-tumor microenvironments. Mol. Cell. Biol. *26*, 5336–5347.

Lamb, C.A., Yoshimori, T., and Tooze, S.A. (2013). The autophagosome: origins unknown, biogenesis complex. Nat. Rev. Mol. Cell Biol. *14*, 759–774.

Levine, B., and Kroemer, G. (2008). Autophagy in the pathogenesis of disease. Cell *132*, 27–42.

Liu, X., Chhipa, R.R., Pooya, S., Wortman, M., Yachyshin, S., Chow, L.M., Kumar, A., Zhou, X., Sun, Y., Quinn, B., et al. (2014). Discrete mechanisms of mTOR and cell cycle regulation by AMPK agonists independent of AMPK. Proc. Natl. Acad. Sci. USA *111*, E435–E444.

Mirguet, O., and Bouillot, A. (2011). Patent WO 2011138307A1 Pyrrolo [3, 2 -d] pyrimidin-3 -yl derivatives used as activators of ampk. http://www.google.com.na/patents/WO2011138307A1?cl=de.

Mizuki, M., Fenski, R., Halfter, H., Matsumura, I., Schmidt, R., Müller, C., Grüning, W., Kratz-Albers, K., Serve, S., Steur, C., et al. (2000). Flt3 mutations from patients with acute myeloid leukemia induce transformation of 32D cells mediated by the Ras and STAT5 pathways. Blood *96*, 3907–3914.

Mizushima, N., Yoshimori, T., and Levine, B. (2010). Methods in mammalian autophagy research. Cell *140*, 313–326.

Nakada, D., Saunders, T.L., and Morrison, S.J. (2010). Lkb1 regulates cell cycle and energy metabolism in haematopoietic stem cells. Nature *468*, 653–658.

Ozcan, U., Yilmaz, E., Ozcan, L., Furuhashi, M., Vaillancourt, E., Smith, R.O., Görgün, C.Z., and Hotamisligil, G.S. (2006). Chemical chaperones reduce ER stress and restore glucose homeostasis in a mouse model of type 2 diabetes. Science *313*, 1137–1140.

Ozcan, U., Ozcan, L., Yilmaz, E., Düvel, K., Sahin, M., Manning, B.D., and Hotamisligil, G.S. (2008). Loss of the tuberous sclerosis complex tumor suppressors triggers the unfolded protein response to regulate insulin signaling and apoptosis. Mol. Cell *29*, 541–551.

Perl, A.E., Kasner, M.T., Tsai, D.E., Vogl, D.T., Loren, A.W., Schuster, S.J., Porter, D.L., Stadtmauer, E.A., Goldstein, S.C., Frey, N.V., et al. (2009). A phase I study of the mammalian target of rapamycin inhibitor sirolimus and MEC chemotherapy in relapsed and refractory acute myelogenous leukemia. Clin. Cancer Res. *15*, 6732–6739.

Scotland, S., Saland, E., Skuli, N., de Toni, F., Boutzen, H., Micklow, E., Sénégas, I., Peyraud, R., Peyriga, L., Théodoro, F., et al. (2013). Mitochondrial energetic and AKT status mediate metabolic effects and apoptosis of metformin in human leukemic cells. Leukemia *27*, 2129–2138.

Shackelford, D.B., Vasquez, D.S., Corbeil, J., Wu, S., Leblanc, M., Wu, C.L., Vera, D.R., and Shaw, R.J. (2009). mTOR and HIF-1alpha-mediated tumor metabolism in an LKB1 mouse model of Peutz-Jeghers syndrome. Proc. Natl. Acad. Sci. USA *106*, 11137–11142.

Shackelford, D.B., Abt, E., Gerken, L., Vasquez, D.S., Seki, A., Leblanc, M., Wei, L., Fishbein, M.C., Czernin, J., Mischel, P.S., and Shaw, R.J. (2013). LKB1 inactivation dictates therapeutic response of non-small cell lung cancer to the metabolism drug phenformin. Cancer Cell *23*, 143–158.

Sheen, J.H., Zoncu, R., Kim, D., and Sabatini, D.M. (2011). Defective regulation of autophagy upon leucine deprivation reveals a targetable liability of human melanoma cells in vitro and in vivo. Cancer Cell *19*, 613–628.

Stewart, S.A., Dykxhoorn, D.M., Palliser, D., Mizuno, H., Yu, E.Y., An, D.S., Sabatini, D.M., Chen, I.S., Hahn, W.C., Sharp, P.A., et al. (2003). Lentivirus-delivered stable gene silencing by RNAi in primary cells. RNA *9*, 493–501.

Sui, X., Chen, R., Wang, Z., Huang, Z., Kong, N., Zhang, M., Han, W., Lou, F., Yang, J., Zhang, Q., et al. (2013). Autophagy and chemotherapy resistance: a promising therapeutic target for cancer treatment. Cell Death Dis. *4*, e838.

Takeuchi, H., Kondo, Y., Fujiwara, K., Kanzawa, T., Aoki, H., Mills, G.B., and Kondo, S. (2005). Synergistic augmentation of rapamycin-induced autophagy in malignant glioma cells by phosphatidylinositol 3-kinase/protein kinase B inhibitors. Cancer Res. *65*, 3336–3346.

Tamburini, J., Green, A.S., Bardet, V., Chapuis, N., Park, S., Willems, L., Uzunov, M., Ifrah, N., Dreyfus, F., Lacombe, C., et al. (2009). Protein synthesis is resistant to rapamycin and constitutes a promising therapeutic target in acute myeloid leukemia. Blood *114*, 1618–1627.

van Galen, P., Kreso, A., Mbong, N., Kent, D.G., Fitzmaurice, T., Chambers, J.E., Xie, S., Laurenti, E., Hermans, K., Eppert, K., et al. (2014). The unfolded protein response governs integrity of the haematopoietic stem-cell pool during stress. Nature *510*, 268–272.

Vázquez, C.L., and Colombo, M.I. (2009). Assays to assess autophagy induction and fusion of autophagic vacuoles with a degradative compartment, using monodansylcadaverine (MDC) and DQ-BSA. Methods Enzymol. *452*, 85–95.

Wang, Q., Mora-Jensen, H., Weniger, M.A., Perez-Galan, P., Wolford, C., Hai, T., Ron, D., Chen, W., Trenkle, W., Wiestner, A., and Ye, Y. (2009). ERAD inhibitors integrate ER stress with an epigenetic mechanism to activate BH3-only protein NOXA in cancer cells. Proc. Natl. Acad. Sci. USA *106*, 2200–2205.

Wiederschain, D., Wee, S., Chen, L., Loo, A., Yang, G., Huang, A., Chen, Y., Caponigro, G., Yao, Y.M., Lengauer, C., et al. (2009). Single-vector inducible lentiviral RNAi system for oncology target validation. Cell Cycle *8*, 498–504.

Xiao, B., Sanders, M.J., Carmena, D., Bright, N.J., Haire, L.F., Underwood, E., Patel, B.R., Heath, R.B., Walker, P.A., Hallen, S., et al. (2013). Structural basis of AMPK regulation by small molecule activators. Nat. Commun. *4*, 3017.

Yeung, J., Esposito, M.T., Gandillet, A., Zeisig, B.B., Griessinger, E., Bonnet, D., and So, C.W. (2010). β-Catenin mediates the establishment and drug resistance of MLL leukemic stem cells. Cancer Cell *18*, 606–618.